



concentrations of PAHs.<sup>6</sup> We were unable to determine sorption to PS because chemical analyses were unsuccessful using a conventional one-dimensional gas chromatography–mass spectrometry (GC–MS) method because of the complexity of the sample matrix. Here, we applied a recently developed method based on comprehensive two-dimensional gas chromatography coupled to time-of-flight mass spectrometry (GC × GC/ToF-MS)<sup>17</sup> to successfully analyze parent-PAHs (PPAHs), alkyl-PAHs (MPAHs), nitro-PAHs (NPAHs), oxy-PAHs (OPAHs), and thio-PAHs (SPAHS) within one single chromatographic run.

Here, we analyzed multiple classes of PAHs on PS pellets deployed in San Diego Bay for up to 1 year to test the hypotheses that (1) PAHs are associated with virgin PS, (2) PAHs will sorb to PS in the marine environment from several sources, and (3) concentrations will differ from other plastic types. This work provides insight into potential hazards associated with PS marine debris. PS is a common marine debris item<sup>18</sup> and has been found in the gut contents of fish.<sup>19</sup> In the absence of PAHs, PS poses a hazard to marine organisms because of its hazardous styrene monomer, both carcinogenic and disruptive to the endocrine system.<sup>20</sup> Here, we show that several PAHs are associated with PS before deployment and, when littered in the marine environment, sorb greater concentrations of these hazardous chemicals. Thus, individual hazards associated with both PS and PAHs make PS marine debris a potential multiple stressor in marine habitats when available for ingestion by marine life.

## EXPERIMENTAL SECTION

**Experimental Design.** PS virgin pre-production plastic pellets (3 mm long and 2 mm in diameter) were deployed from floating docks in San Diego Bay.<sup>6</sup> Here, we focus on two locations (see Figure S1 of the Supporting Information): San Diego Harbor Excursions in the central bay and Shelter Island near the mouth of the bay. Details regarding experimental design can be found in the study by Rochman et al.<sup>6</sup> Briefly, at each location, two replicate samples were deployed for collection at the end of five time periods: 1, 3, 6, 9, and 12 months (20 total samples). Each replicate consisted of 5 g of pellets in individual Nitex mesh (1.3 mm) bags within a nylon mesh (10 mm) bag. Replicate samples were deployed by hanging each nylon bag on one of two identical PVC frames suspended from each dock (approximately 2 m from each other and at a depth approximately 0.5 m below the surface). At the end of their randomly assigned deployment time, samples were collected and stored at  $-20\text{ }^{\circ}\text{C}$  until analysis. We also analyzed three replicate samples of virgin pellets never deployed in the bay (i.e., 0 month samples). Methods for preparing samples for chemical analyses were established previously in our laboratory<sup>8</sup> and are described by Rochman et al.<sup>6</sup> For more information regarding chemical standards and solvent materials, sample prep, chemical analyses, and quality assurance (QA)/quality control (QC) refer to the Supporting Information.

**GC × GC/ToF-MS Analysis for PAHs.** A GC × GC/ToF-MS Pegasus 4D (LECO, St. Joseph, MI) equipped with an Agilent 6890 GC with a secondary oven, a split/splitless injector, and a non-moving quad-jet dual-stage modulator was used. Two GC columns, LC-50 (10 m × 0.15 mm × 0.10  $\mu\text{m}$ ) in the first dimension and NSP-35 (1.2 m × 0.10 mm × 0.10  $\mu\text{m}$ ) in the second dimension (J&K Scientific, Edwardsville, Nova Scotia, Canada) were connected using an Agilent CPM union (part 188-5361) for 0.1–0.25 mm inner diameter columns. The

data processing was performed using ChromaTOF, version 4.33. The optimization parameters are described in previous studies,<sup>17,21–24</sup> and optimized conditions are described in Table S1 of the Supporting Information. Five-point calibration curves with a range of 5–1000 pg/ $\mu\text{L}$  were used, using the same approach that has been described previously.<sup>24</sup>

**Statistical Methods.** We quantified temporal patterns by fitting a first-order approach to an equilibrium model<sup>25</sup> when concentrations appeared to be increasing and an exponential decay model when concentrations appeared to be decreasing.<sup>26</sup> SigmaPlot 10 (SYSTAT Software, Chicago, IL) was used to fit the exponential rise to maximum,  $C_t = C_{\text{eq}}(1 - e^{-kt})$ , and exponential decay,  $C_t = (C_0 - C_{\text{eq}})e^{-kt} + C_{\text{eq}}$ , equations, where  $C_t$  is the concentration at time  $t$ ,  $C_{\text{eq}}$  is the predicted equilibrium concentration,  $C_0$  is the initial concentration, and  $k$  is the rate constant. We examined spatial patterns using principle component analysis (PCA) run with IBM SPSS, version 19, and potential sources using molecular ratios of several PAHs at each location. This method involves comparing concentration ratios of frequently found PAHs to identify possible sources<sup>27</sup> and should be used with caution because molecular ratios can easily be altered by different factors, such as reactivity of PAHs and degradation.<sup>27–29</sup> The combination of five molecular ratios containing fluorene (FLO), pyrene (PYR), anthracene (ANT), phenanthrene (PHE), benzo[*a*]pyrene (BaP), chrysene (CHR), benz[*a*]anthracene (BaA), triphenylene (TRI), benzo[*b*]fluoranthene (BbF), and benzo[*k*]fluoranthene (BkF) were used to generate bivariate plots (Figure 5).<sup>30–33</sup> Two-sample student  $t$  tests run in SigmaPlot 10 (SYSTAT Software, Chicago, IL) determined if concentrations of PAHs and molecular ratios were statistically different between locations. Concentrations of total sorbed PPAHs were log-transformed to achieve normality. We tested for differences among plastic types and locations in San Diego Bay by performing a two-factor analysis of variance (ANOVA) on data from each sampling period individually with SYSTAT 12 (SYSTAT Software, Chicago, IL). Data for PPAHs sorbed to HDPE, LDPE, PP, PET, and PVC deployed simultaneously with PS were included in this analysis.<sup>6</sup> Homogeneity of variance was verified by Levene's test. Post-hoc Tukey's tests were used to distinguish significantly different treatment means.

## RESULTS AND DISCUSSION

**PAH Analysis Achieved by the GC × GC/ToF-MS Method.** The one-dimensional GC–MS method<sup>6</sup> previously used for analysis of PAHs in other plastic types was unsuccessful for the PS samples. The column was sacrificed because of column overload and strong matrix interferences that can be seen as very large peaks eluting at the beginning of the run in the selected ion monitoring (SIM) chromatogram (Figure 1). The inner boxes in Figure 1 show PAHs co-eluting with interfering components represented by large peaks that do not correspond to any PAH or internal standard.

Figure 2 shows the total ion chromatogram (TIC) for the analysis of a PS sample using the GC × GC/ToF-MS method developed for simultaneous analysis of multiple groups of PAHs,<sup>17,24</sup> where the sample matrix (represented by dashed lines) elutes in regions that do not interfere with most of the PAHs (represented by a dotted line). This two-dimensional method was successful to analyze a total of 85 PAHs for identification and quantitation in PS samples, including 18 PPAHs, 9 MPAHs, 15 CIPAHS, 6 BrPAHs, 17 OPAHs, and 2 SPAHS (see Table S2 for a complete list of targeted PAHs).

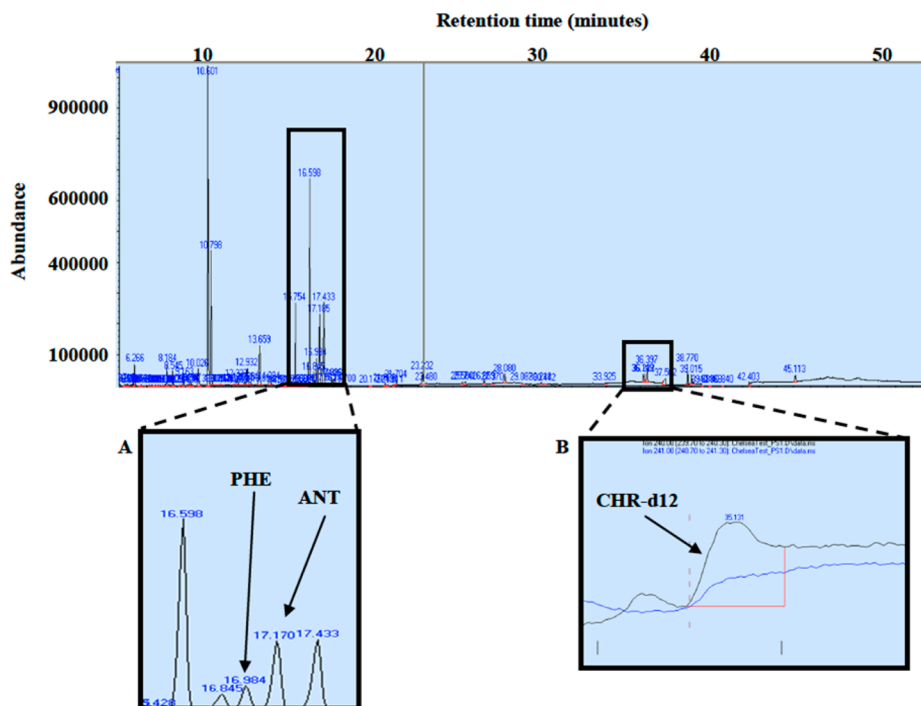


**Figure 1.** One-dimensional chromatogram of the sum of selected ions for a PS extract analyzed using a 30 m DB-5 column after solid-phase extraction (SPE). The inner boxes show some of the PAHs with co-elution problems. (A) Phenanthrene (PHE) and anthracene (ANT) co-eluting with interfering components represented by large peaks that do not correspond to PAHs or internal standards. (B) Chrysene-*d*<sub>12</sub> (CHR-*d*<sub>12</sub>) showing peak broadening and baseline drifting possibly because of matrix co-eluting with the target compound.

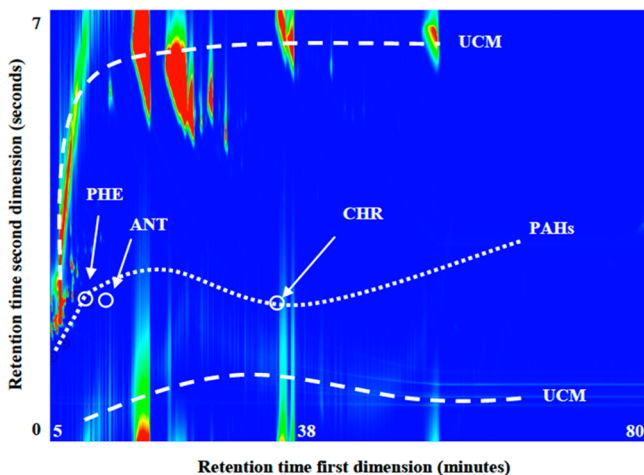


**Figure 2.** GC  $\times$  GC/ToF-MS contour map of the TIC for a PS extract. The *x* axis represents the retention time in the first dimension (min), and the *y* axis represents the retention time in the second dimension (s). The dotted line represents the elution profile for the PAHs in the sample, which is isolated from most of the sample matrix, and the unresolved complex mixture (UCM) is represented by the dashed line below and above the PAHs line. PAHs that had co-elution problems when using a one-dimensional GC are labeled: phenanthrene (PHE), anthracene (ANT), and chrysene (CHR).

**PAHs in PS.** A total of 25 PAHs (15 PPAHs, 7 MPAHs, 2 OPAHs, and 1 SPAH) were detected in the PS samples. Table 1 shows the concentrations of all PAHs detected (in ng/g) at each sampling period (0, 1, 3, 6, 9, and 12 months) from each location. Congeners from each group were found in virgin PS pellets before deployment. Of the PPAHs, acenaphthene, acenaphthylene, anthracene, fluoranthene, fluorene, phenanthrene,

and pyrene were found in virgin PS pellets. These seven PAHs have the lowest molecular weight (MW) of the PPAHs targeted and have a log  $K_{ow}$  (octanol–water partitioning coefficient) less than or equal to 5. Low-molecular-weight PAHs are characterized to come from direct petrogenic sources,<sup>34</sup> including the raw material petroleum. Of the MPAHs, 1,3-dimethylnaphthalene, 2,6-dimethylnaphthalene, 1-methylphenanthrene, and 2-methylphenanthrene were found in virgin PS pellets. MPAHs are an associated byproduct of petroleum emissions.<sup>35</sup> Both OPAHs, 9-fluorenone and 1,4-naphthoquinone, were measured in virgin PS pellets and can be formed from the incomplete combustion of organic material,<sup>36</sup> including petroleum. Dibenzothiophene, also found in virgin PS pellets, occurs naturally in the production of oil.<sup>37</sup> Because PAHs are associated with petroleum, the raw material of plastics, this is expected.

The detection of PAHs in virgin PS pellets adds additional information to previous work showing that PS virgin pellets have up to 2 orders of magnitude greater concentrations of PPAHs than other polymers.<sup>8</sup> When PAHs in virgin PS pellets quantified here are compared to those measured in other types of plastics by Rochman et al.,<sup>6</sup> we find that PPAHs in virgin pellets range from nd to 2 ng/g in PVC, from nd to 1 ng/g in PET, from 2 to 6 ng/g in PP, from 3 to 6 ng/g in HDPE, and from nd to 13 ng/g in LDPE; however, in virgin PS pellets, PPAHs range from 79 to 97 ng/g ( $n = 3$ ), approximately 8–200 times greater than other polymers. This large difference in PPAHs in PS virgin pellets strengthens our hypothesis that PAHs are associated with the manufacturing process, likely related to the aromaticity of the styrene monomer.<sup>8,38</sup>

PAH formation may arise from multiple stages in the life cycle of PS. To manufacture PS, ethylene and benzene are produced from crude oil under applied heat.<sup>39</sup> The styrene monomer is contrived by reacting benzene with ethylene to

**Table 1. Concentration of PAHs Found in PS Pellets (in ng/g) Deployed for 0, 1, 3, 6, 9, and 12 Months in Harbor Excursion and Shelter Island Sampling Sites, Determined Using GC × GC/ToF-MS**

months	Harbor Excursion						Shelter Island															
	0 (blank)		1 month		3 months		6 months		9 months		12 months											
	mean (n = 3)	SD	n = 2	n = 2	n = 2	n = 2	n = 2	n = 2	n = 2	n = 2	n = 2	n = 2										
1,3-dimethylnaphthalene	24.3	4.24	29.8	17.9	22.9	23.1	15.4	22.3	18.2	17.4	17.8	14.8	18.5	21.7	17.0	17.8	14.9	14.8	9.64	12.3	13.4	8.93
1-methylphenanthrene	12.2	0.18	29.2	16.6	17.2	16.0	16.4	15.1	19.3	16.9	18.1	17.1	13.2	13.9	13.4	13.6	14.5	12.7	14.5	12.9	13.4	13.7
1-methylpyrene	nd <sup>a</sup>	0	17.6	16.2	16.3	21.0	15.6	14.9	17.5	18.1	16.3	17.8	nd									
2,6-dimethylnaphthalene	9.30	0.5	8.33	6.67	6.73	7.33	6.56	8.21	6.83	6.26	6.94	6.92	7.45	7.98	6.51	6.90	6.30	6.04	6.30	5.67	5.97	5.75
2-methylanthracene	nd	0	17.0	18.4	17.3	16.7	17.9	15.8	18.9	18.7	18.1	18.9	13.8	14.1	13.9	15.2	13.7	15.1	15.1	14.5	14.9	15.0
2-methylphenanthrene	13.5	0.15	19.7	15.5	15.6	15.5	15.1	14.5	15.9	15.8	15.3	13.9	13.9	14.0	14.1	13.9	14.2	13.4	14.4	13.4	13.9	13.8
triphenylene	nd	0	10.9	8.60	8.63	7.56	8.82	6.32	9.23	9.68	8.09	10.2	5.84	5.41	5.38	5.59	6.33	5.65	6.32	5.65	6.53	6.71
∑MPAHs	59.2	4.71	132	99.9	105	107	95.9	97.1	105	103	101	101	72.6	77.1	70.3	71.7	71.4	66.1	66.3	64.4	68.1	63.9
acenaphthene	5.23	0.49	38.7	13.3	13.5	14.8	14.6	13.2	15.2	14.2	15.5	14.0	5.40	5.66	6.19	5.93	5.73	5.45	6.21	5.41	5.81	5.96
acenaphthylene	6.76	0.83	18.7	19.3	15.8	17.8	22.8	13.9	18.8	22.8	18.7	22.1	9.33	9.74	9.80	10.4	11.2	10.3	15.2	10.6	11.1	13.3
anthracene	5.41	0.14	44.1	42.2	40.1	39.2	43.8	25.4	45.9	53.5	44.3	49.4	10.1	10.6	11.0	13.7	15.6	14.3	18.1	13.5	16.7	18.1
benzo[ <i>a</i> ]anthracene	nd	nd	34.2	21.2	17.6	17.1	18.9	12.5	21.2	18.3	16.0	19.6	6.08	6.95	6.32	7.29	8.51	6.73	8.67	7.51	7.85	9.91
benzo[ <i>a</i> ]pyrene	nd	nd	24.0	21.4	18.9	19.2	17.1	13.5	16.6	24.7	16.1	18.2	6.42	7.76	7.17	8.32	9.48	7.58	11.3	8.99	9.62	10.3
benzo[ <i>b</i> ]fluoranthene	nd	nd	33.0	35.0	44.2	35.0	38.8	22.6	35.7	40.0	27.7	31.5	12.0	13.5	13.8	15.0	19.0	15.4	18.6	18.1	16.6	22.1
benzo[ <i>c</i> ]pyrene	nd	nd	24.9	25.1	22.8	23.1	25.2	14.5	22.0	33.6	20.7	22.6	8.78	9.41	9.32	10.7	12.6	10.3	13.7	14.5	11.7	14.9
benzo[ <i>ghi</i> ]perylene	nd	nd	nd	38.0	36.6	36.3	40.0	33.6	38.6	41.9	37.9	37.5	34.3	34.2	34.8	33.8	35.5	33.1	34.9	34.8	34.4	34.6
benzo[ <i>k</i> ]fluoranthene	nd	nd	21.7	23.3	27.9	23.2	23.1	15.9	21.7	23.3	17.4	20.2	9.43	8.73	8.54	10.6	11.9	10.2	11.3	10.6	10.8	11.9
chrysene	nd	nd	33.9	20.9	18.7	20.0	19.2	11.7	22.0	23.6	15.4	23.5	7.45	7.30	7.50	7.72	9.25	7.49	9.09	7.55	8.36	11.8
fluoranthene	23.0	13.6	126	33.2	41.6	35.2	39.4	24.8	46.4	36.0	33.5	43.9	18.4	19.5	18.3	19.4	21.7	18.2	25.7	21.3	23.0	26.1
fluorene	25.4	3.41	74.0	40.1	48.3	54.1	37.2	43.2	38.8	43.1	47.1	46.5	31.6	36.8	25.6	38.9	31.5	34.9	40.6	32.1	24.0	30.1
indeno[1,2,3- <i>cd</i> ]pyrene	nd	nd	30.4	33.7	33.8	32.6	34.3	27.7	33.2	39.6	32.9	32.4	27.6	28.4	27.9	29.8	30.6	27.9	28.0	29.2	29.8	30.7
phenanthrene	12.6	0.64	208	74.2	68.9	70.8	67.1	105	96.4	141	96.9	113	63.0	71.1	85.8	126	133	127	82.3	89.6	98.4	109
pyrene	15.7	6.42	203	55.5	74.6	59.5	68.3	21.0	73.0	57.5	58.9	68.4	17.8	22.0	14.5	15.1	22.9	17.7	13.6	20.2	17.4	27.6
∑PPAHs	94.2	14.5	915	496	523	498	510	398	545	613	499	563	268	292	286	353	378	347	337	324	325	376
9-fluorenone	7.90	1.2	10.0	10.1	10.5	11.2	9.08	10.5	10.8	10.6	12.9	12.0	9.63	10.9	9.47	9.64	12.0	9.83	11.0	8.97	9.11	11.1
1,4-naphthoquinone	45.4	0.79	47.0	45.9	47.8	47.5	46.6	45.8	47.4	48.0	48.7	47.8	46.9	46.7	45.6	46.7	46.9	44.0	48.8	46.0	46.5	51.1
∑OPAHs	53.3	1.93	57.0	56.0	58.3	58.7	55.7	56.3	58.2	58.6	61.6	59.8	56.5	57.6	55.1	56.3	58.9	53.9	59.8	54.9	55.6	62.2
dibenzothiophene	4.35	0.06	19.3	6.90	7.41	7.30	6.19	5.99	7.40	6.92	7.13	7.02	3.98	3.99	3.87	4.01	4.08	3.92	4.15	3.93	3.97	4.03
∑SPAHs	4.35	0.06	19.3	6.90	7.41	7.30	6.19	5.99	7.40	6.92	7.13	7.02	3.98	3.99	3.87	4.01	4.08	3.92	4.15	3.93	3.97	4.03
total PAHs	211	21	1120	659	694	671	667	558	716	782	669	730	401	430	416	485	512	470	468	447	453	506

<sup>a</sup>nd = compound not detected.

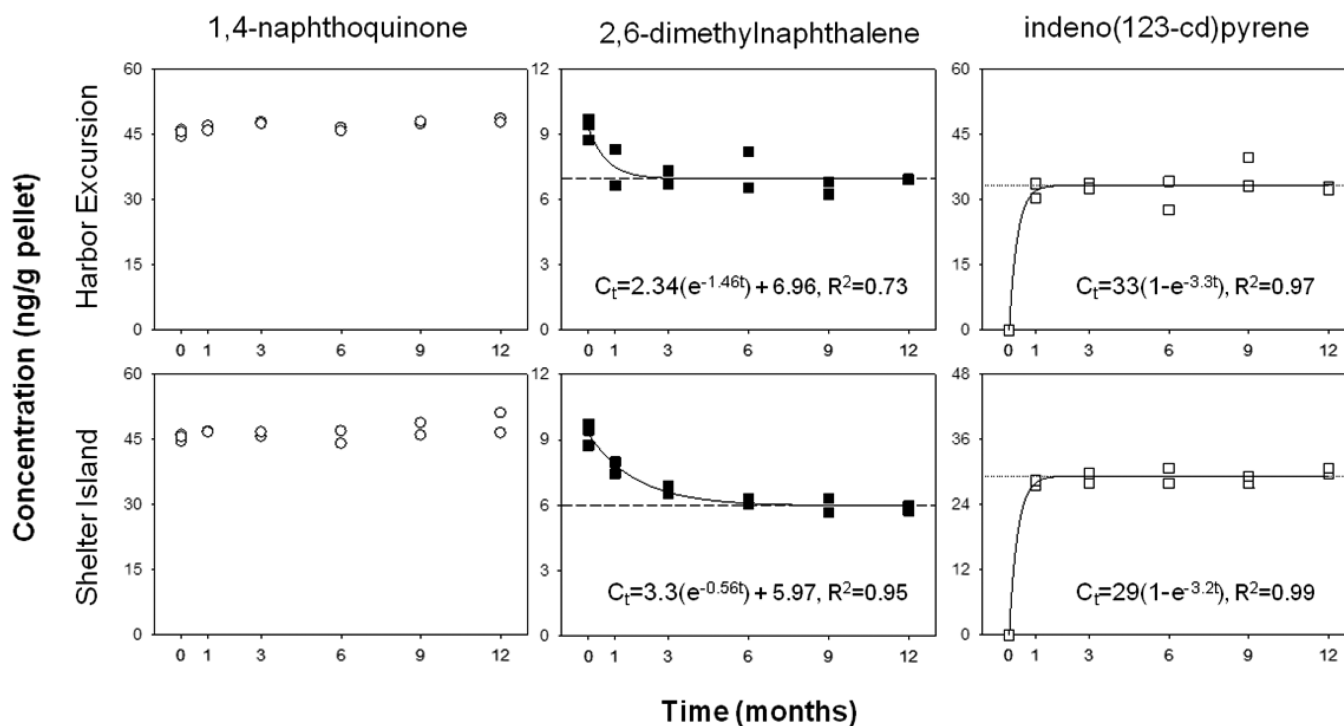


**Figure 3.** Concentrations of 1,4-naphthoquinone (no change over time; left), 2,6-dimethylnaphthalene (decreasing over time; middle), and indeno(123-cd)pyrene (increasing over time; right) in ng/g of pellets versus time for PS at Harbor Excursion (top rows) and Shelter Island (bottom rows). Please note that vertical axes differ among graphs. Data were fit to the first-order approach to an equilibrium model<sup>25</sup> using the exponential rise to the maximum equation  $C_t = C_{eq}(1 - e^{-kt})$  or the exponential decay model<sup>26</sup> using the equation  $C_t = (C_0 - C_{eq})e^{-kt} + C_{eq}$ , where  $C_t$  is the concentration at time  $t$ ,  $C_{eq}$  is the predicted equilibrium concentration,  $C_0$  is the initial concentration, and  $k$  is the rate constant. The horizontal dotted line denotes the predicted  $C_{eq}$  for each plastic type. Where the equation and lines are missing, the data could not be fit to the equation.

make ethyl benzene, which is dehydrogenated to styrene at 550–680 °C.<sup>39</sup> Both benzene and styrene are precursors of PAH formation.<sup>40</sup> Once polymerized, PS is more capable of depolymerizing into its individual monomers than other polymers,<sup>20</sup> and because polymerization reactions are rarely complete, the residual monomer styrene is likely to be found in the polymeric product.<sup>20</sup> Thus, the monomer styrene is likely available for PAH formation during and post-manufacturing. Once PS pre-production pellets are produced, manufacturers apply heat again to process and shape end products from PS pellets,<sup>39</sup> likely resulting in emissions of more PAHs. Lastly, combustion of PS waste products results in greater PAH emissions than other polymers.<sup>41</sup>

Temporal patterns among individual congeners of PAHs were examined to better understand PS as a source and sink for PAHs in the marine environment. We quantified temporal patterns by fitting a first-order approach to an equilibrium model<sup>25</sup> when concentrations of PAHs increased over time and an exponential decay model when concentrations decreased.<sup>26</sup> Fitting these equations assumes a relatively constant background concentration of PAHs. Although this assumption likely does not hold during a field deployment, the equations fit our data relatively well over the long time scales of our experiment, despite temporal variability. Where concentrations of PAHs were relatively constant during deployment, neither model could be fit. Because sorption is related to the hydrophobicity of each specific congener, we quantified temporal patterns for individual PAHs sorbed to PS at each location (see Figure 3 and Figures S2 and S3 of the Supporting Information). To compare sorption trends of PS analyzed here to HDPE, LDPE, PP, PET, and PVC analyzed previously,<sup>6</sup> we also quantified

temporal patterns for sorption of total priority PPAHs at Harbor Excursion, where concentrations are greatest (see Figure S4 of the Supporting Information).

We observed PS behaving as a source or a sink for several PAH congeners in San Diego Bay. However, for some congeners, we did not observe PS behaving as either. Concentrations of 1-methylphenanthrene, 2-methylphenanthrene, 9-fluorenone, 1,4-naphthoquinone, dibenzothiophene, fluorene, and fluoranthene remained relatively constant over time (see Figure 3 and Figures S2 and S3 of the Supporting Information). Concentrations of 1,3-dimethylnaphthalene and 2,6-methylnaphthalene decreased upon deployment (see Figure 3 and Figures S2 of the Supporting Information), suggesting that PS may be a source of these PAHs to the marine environment. While these low-molecular-weight two-ring PAHs do have a greater solubility in water than other PAH congeners, another explanation may be that these compounds underwent degradation as a result of exposure to sunlight and/or marine microorganisms. We observed PS behaving as a sink for several PAHs measured in this study, including 1-methylpyrene, 2-methylanthracene, and all measured PPAHs, except fluorene and fluoranthene (see Figure 3 and Figures S2 and S3 of the Supporting Information). At Harbor Excursion, where concentrations of PAHs were greatest, these PAHs fit the first-order kinetics model well, whereas at Shelter Island, sorption trends for 1-methylpyrene (not detected), acenaphthylene, acenaphthene, and pyrene could not be fit to the equation.

For PAHs sorbed to PS from ambient seawater, we expected individual congeners to behave differently, because chemicals with less hydrophobicity and a lighter MW are expected to reach saturation faster than those with greater hydrophobicity and a heavier MW.<sup>42</sup> While we observed this for PPAHs

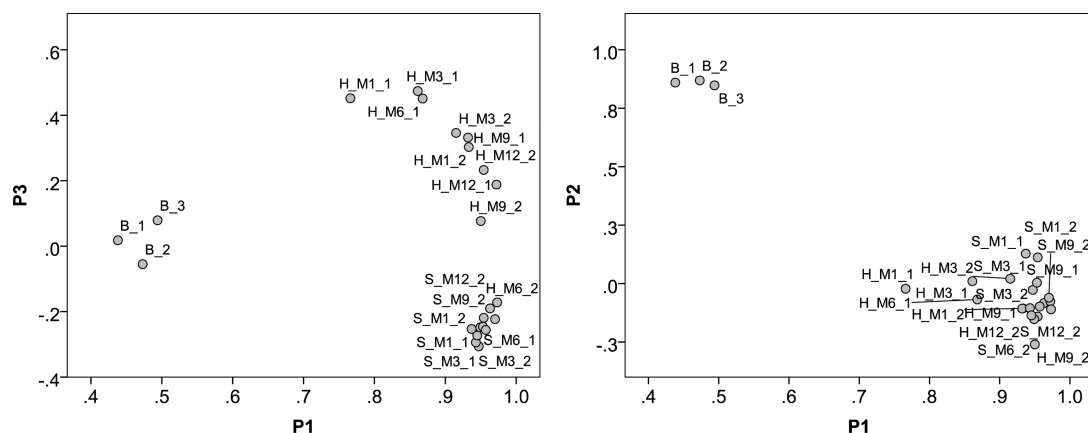


**Figure 4.** PCA of the concentration of PAHs. Three principal components are shown. Generalized grouping: B, blank, virgin PS pellets not deployed; H\_M, Harbor Excursion sampling site, with 1, 3, 6, 9, and 12 months of exposure; and S\_M, Shelter Island sampling site, with 1, 3, 6, 9, and 12 months of exposure.

sorbing to HDPE, LDPE, and PP at Harbor Excursion,<sup>6</sup> similar to PET and PVC,<sup>6</sup> we did not see obvious differences in sorption patterns among individual congeners for PS at either location (see Figure S3 of the Supporting Information). Differences in sorption patterns among congeners may not be expected for the glassy polymers, PET, PVC, and PS, where diffusion into the polymer is not expected.<sup>43</sup> Thus, these polymers may exhibit a relatively rapid adsorption onto the surface that is not followed by a slower diffusion into the polymeric matrix, as is expected for polyethylene.<sup>42</sup>

While sorbed concentrations of total PPAHs on PS are similar to HDPE and LDPE, the time to reach predicted equilibrium happens much faster (see Figure S4 of the Supporting Information). After the 1 month sampling period, concentrations of total PPAHs sorbed to PS changed little over time at both locations (Table 1). Temporal patterns for PS at Harbor Excursion are similar to what is observed for PET and PVC.<sup>6</sup> In contrast, at this location, HDPE, LDPE, and PP reached their predicted equilibriums by 6 months.<sup>6</sup> Thus, the relatively large concentrations of PPAHs sorbing to PS occur relatively quickly after deployment into the marine environment (see Figure S4 of the Supporting Information). Management of PS may hold a greater priority than debris composed of HDPE, LDPE, PP, PET, or PVC because our data suggest that PS acquires relatively large concentrations of hazardous chemicals after a short period of time at sea.

**Site Difference for PAHs.** Total PAH concentrations were greater at Harbor Excursion compared to Shelter Island by a factor of approximately 2 (Table 1). Concentrations of 21 of the 25 individual PAHs quantified were significantly greater ( $p < 0.05$ ) at Harbor Excursion than Shelter Island, whereas 2,6-dimethylnaphthalene, phenanthrene, 9-fluorenone, and 1,4-naphthaquinone were not statistically different ( $p > 0.05$ ) between locations. Concentrations of these four PAHs, with the exception of phenanthrene, decreased or did not change over time. Significant differences among the remaining PAHs are probably related to different sources of contamination between locations.

Parts a and b of Table S3 of the Supporting Information show the PAH compositional difference (%) of the two locations compared to the virgin blanks (0 month exposure). The PAH composition of each sample was compared using PCA because of the many variables (25 PAHs). The analysis shows that the top three components (P1–P3) explain 97% of

the variance, with P1 = 79%, P2 = 11%, and P3 = 7.5%. The PAH composition of the virgin PS pellets was clearly different from the deployed PS pellets (Figure 4). Among the deployed PS pellets, the PAH composition was slightly different between the two sites, except one sample from Harbor Excursion (sampled at 6 months; Figure 4). Differences in PAH compositions suggest different sources of PAHs.

To further examine sources of PAHs at each location, we used molecular ratios. The FLO/(FLO + PYR) ratio was significantly different between sites ( $p < 0.001$ ), averaging 0.421 ( $\pm 0.106$ ) at Harbor Excursion and 0.633 ( $\pm 0.067$ ) at Shelter Island, suggesting a gasoline origin for PAHs at Harbor Excursion and a diesel origin for PAHs at Shelter Island (Figure 5A). The ANT/(ANT + PHE) ratio was also significantly different between sites ( $p < 0.001$ ), averaging 0.307 ( $\pm 0.073$ ) for Harbor Excursion and 0.128 ( $\pm 0.025$ ) for Shelter Island, suggesting a pyrogenic origin for PAHs at Harbor Excursion and a more petrogenic origin at Shelter Island (panels A, B, and D of Figure 5), which is reinforced by the ratio BaA/(BaA + CHR + TRI) that was also significantly different between locations ( $p < 0.001$ ), averaging 0.397 ( $\pm 0.023$ ) for Harbor Excursion and 0.346 ( $\pm 0.015$ ) for Shelter Island (Figure 5C). The two ratios BbF/BkF and BaP/(BaP + CHR) were not significantly different between locations. These results suggest that PAHs at Shelter Island and Harbor Excursion come from different sources, with Shelter Island showing ratios closer to those found in petroleum and Harbor Excursion showing ratios closer to those found in the generation of pyrogenic PAHs. The suggestion that sources of PAHs to Harbor Excursion are more pyrogenic in origin is further confirmed by our data. For example, dibenzothiophene and 1-methylpyrene, with greater concentration at Harbor Excursion, are indicators of fossil fuels, such as gasoline or diesel exhaust.<sup>44,45</sup> In addition, MPAHs are indicative of direct petroleum emissions,<sup>35</sup> and we found greater concentrations of 1-methylpyrene and 2-methylanthracene at Harbor Excursion relative to Shelter Island likely because of the greater shipping activity at Harbor Excursion.

**PPAH Concentrations in PS Compared to Other Mass-Produced Polymers.** Upon comparing sorbed concentrations of PPAHs in PS to HDPE, LDPE, PP, PET, and PVC previously reported, we found similar patterns confirming our past results, showing that HDPE and LDPE sorb significantly greater PAHs than PP, PET, and PVC and that PP sorbs an intermediate concentration.<sup>6</sup> The inclusion of PS in a two-factor ANOVA for each sampling period reveals a consistently

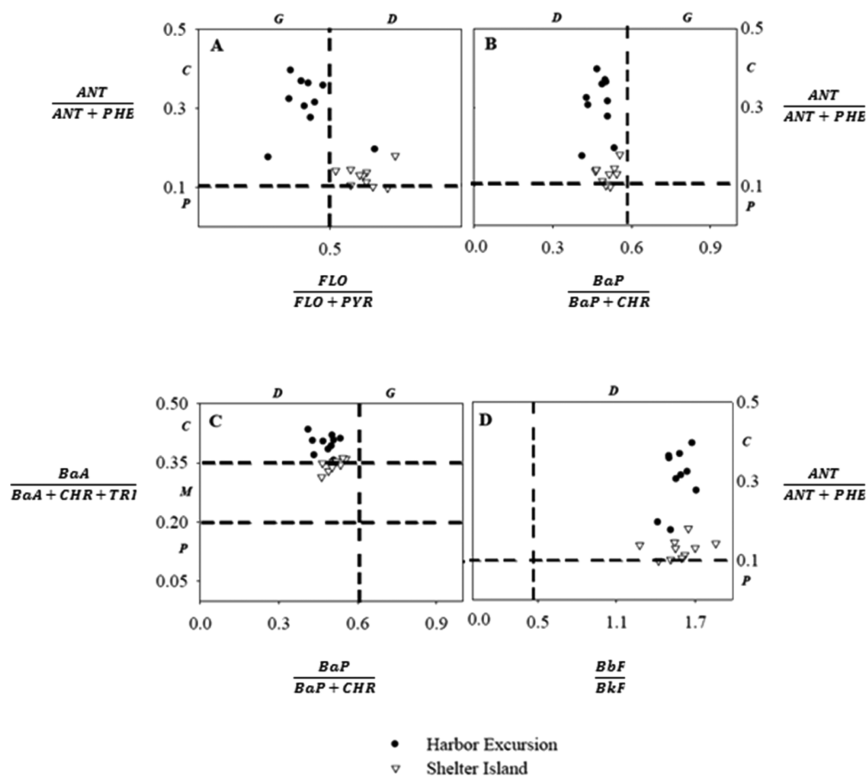


**Figure 5.** Bivariate plots of PAH diagnostic ratios for PS pellets deployed in both sampling sites. (A) FLO/(FLO + PYR) versus ANT/ (ANT + PHE), (B) BaP/(BaP + CHR) versus ANT/(ANT + PHE), (C) BaP/(BaP + CHR) versus BaA/(BaA + CHR + TRI), (D) BbF/BkF versus ANT/ (ANT + PHE). Dashed lines represent threshold values, and letters in italics represent possible sources: G = gasoline, D = diesel, C = combustion of petroleum derivatives, P = PAHs from petroleum, and M = mix sources.

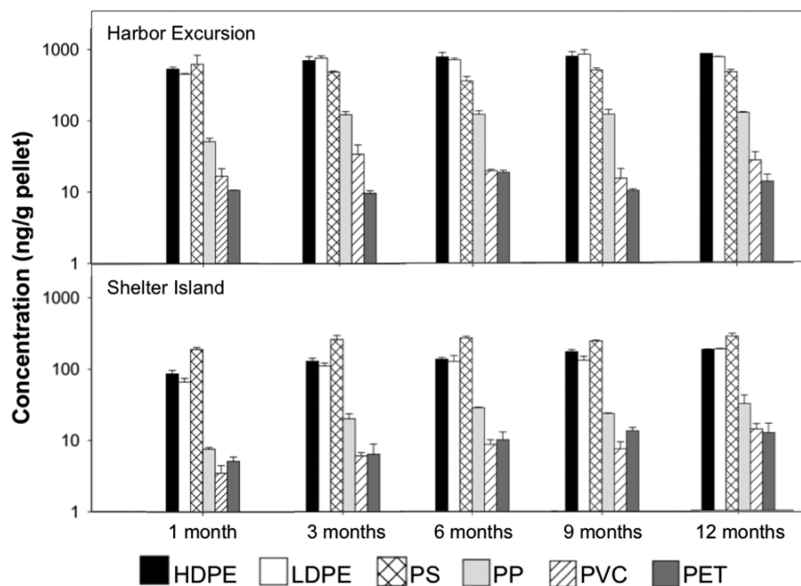


**Figure 6.** Mean concentrations [ $\pm$ standard error (SE)] of  $\Sigma$ PPAHs (ng/g) sorbed to each plastic type at each location during each sampling period (1, 3, 6, 9, and 12 months;  $n = 2$ ). Harbor Excursion (HE site) is shown on the top, and Shelter Island (SI site) is shown on the bottom. At each sampling period, two-factor ANOVA showed significant differences among plastic types ( $p < 0.001$ ) and locations ( $p < 0.001$ ), and post-hoc Tukey comparisons consistently distinguished HDPE, LDPE, and PS as a group of plastics with the largest PPAH concentrations and PET and PVC as a group of plastics with the smallest PPAH concentrations.

significant interaction ( $p < 0.05$ ) between location and plastic type. Still, over space and time, HDPE, LDPE, and PS consistently sorb the greatest concentration of PPAHs. At Shelter Island, PS sorbs the greatest concentration of PPAHs overall, but at Harbor Excursion, differences among HDPE, LDPE, and PS are less conspicuous (Figure 6).

Sorption of PPAHs to PS is relatively large (up to 925.6 ng/g; Table 1) when comparing among the other five most commonly produced polymers (HDPE, LDPE, PP, PET, and PVC).<sup>16</sup> This result may be unexpected on the basis of the physical nature of PS. Non-expanded PS pellets are in a glassy state, similar to PET and PVC, suggesting a lower diffusivity than polyethylene, a rubbery

polymer.<sup>43</sup> Moreover, the polymeric backbone of PS has a benzene molecule where polyethylene has a hydrogen, restricting segmental mobility within the PS chains.<sup>43</sup> In contrast, the presence of benzene increases the distance between adjacent polymeric chains, which can make it easier for a chemical to diffuse into the polymer.<sup>43</sup> Therefore, although polyethylene has greater segmental mobility than PS, PS has a greater distance between polymeric chains and may explain why we observed similar concentrations of PAHs in PS as we did in polyethylene. Moreover, PS foam is one of the most common materials used for SPE<sup>46</sup> because of the contribution of  $\pi$ - $\pi$  and strong hydrophobic interactions to retention,<sup>47</sup> suggesting that environmental sorption to PS may be large, specifically for aromatic compounds, such as PAHs. Because several factors influence the uptake of a compound to a polymer, including physical and chemical properties of the chemical sorbent, measuring sorption of other groups of chemicals to PS is recommended.

**Hazards of PS Littered in Habitats.** The mixture of several PAHs, including oxy-, methyl- and thio-PAHs, in virgin PS pellets may pose a risk to organisms immediately upon being discarded into marine habitats because of the mixture of PAHs in the absence of environmental sorption and its carcinogenic and potentially endocrine-disrupting styrene monomer.<sup>20</sup> Thus, it is important to consider risks to terrestrial and aquatic wildlife from PS litter. In addition, the combination of greater PAHs on virgin PS pellets and relatively large concentrations of sorbed PAHs from ambient seawater suggests that PS may pose a greater risk of exposure to PAHs when it is ingested by marine animals than the other most commonly produced plastic types (HDPE, LDPE, PP, PET, and PVC). Future work should measure sorption of other priority pollutants [e.g., polychlorinated biphenyls (PCBs) and metals] to PS. The mixture of the PS monomer itself, chemicals from the manufacturing process, and those sorbed from the environment may act as a multiple stressor to several species<sup>19,48</sup> that ingest PS debris. Testing this theory requires additional research that measures adverse health effects from dietary exposure of virgin PS and PS deployed in the marine environment to organisms.

## ■ ASSOCIATED CONTENT

### ● Supporting Information

GC  $\times$  GC/ToF-MS optimized parameters (Table S1), list of PAHs targeted by GC  $\times$  GC/ToF-MS (Table S2), percent distribution of PAHs on PS at Harbor Excursion and Shelter Island (parts a and b of Table S3), map of our study sites in San Diego Bay (Figure S1), time trends for MPAHs, OPAHs, and SPAHs over time (Figure S2), PPAHs over time (Figure S3), and total PPAHs over time for each of the six major polymer types (Figure S4). This material is available free of charge via the Internet at <http://pubs.acs.org>.

## ■ AUTHOR INFORMATION

### Corresponding Author

\*E-mail: [ehoh@mail.sdsu.edu](mailto:ehoh@mail.sdsu.edu).

### Present Addresses

§Chelsea M. Rochman: Aquatic Health Program, University of California, Davis, California 95616, United States.

†Carlos Manzano: Canada Centre for Inland Waters, Burlington, Ontario L7S 1A1, Canada.

### Author Contributions

†Chelsea M. Rochman and Carlos Manzano contributed equally to this manuscript.

## Notes

The authors declare no competing financial interest.

## ■ ACKNOWLEDGMENTS

This material is based on work supported by SoCal SETAC, PADI Foundation, SDSU Division of Research Affairs, National Science Foundation Grant 0548190, and a National Science Foundation Graduate Research Fellowship (Grant 2010101195). This publication was made possible in part by Grant P30ES00210 from the National Institute of Environmental Health Sciences (NIEHS), National Institutes of Health (NIH), NIEHS Grant P42 ES016465, and the National Science Foundation (ATM-0841165). The American Chemistry Council donated virgin plastic pellets. The authors thank Harbor Excursion and Michelson Yachts at Shelter Island for donating dock space. S. Kaye and M. Oei assisted with chemical analyses, and Z. Schakner, S. Wheeler, M. Colvin, C. Mazloff, J. Barr, M. Moore, and S. Celustka assisted in the field. The authors thank K. Watanabe for assistance with Figure S1 of the Supporting Information, G. Cherr for advising on experimental design, and A. J. Underwood for advice regarding statistical analyses. The authors thank the analytical chemistry core of Oregon State University's Superfund Research Program for supplying standards and Prof. Takeshi Ohura at the University of Shizouka in Shizouka, Japan, for supplying CIPAH and BrPAH standards. Its contents are solely the responsibility of the authors and do not necessarily represent the official view of the NIEHS, NIH.

## ■ REFERENCES

- (1) Browne, M. A.; Crump, P.; Niven, S. J.; Teuten, E. L.; Tonkin, A.; Galloway, T.; Thompson, R. C. Accumulations of microplastic on shorelines worldwide: Sources and sinks. *Environ. Sci. Technol.* **2011**, *45*, 9175–9179.
- (2) Law, K. L.; Moret-Ferguson, S.; Maximenko, N. A.; Proskurowski, G.; Peacock, E. E.; Hafner, J.; Reddy, C. M. Plastic accumulation in the North Atlantic subtropical gyre. *Science* **2010**, *329*, 1185–1188.
- (3) Goldberg, E. D. Plasticizing the seafloor: An overview. *Environ. Technol.* **1997**, *18*, 195–201.
- (4) Hirai, H.; Takada, H.; Ogata, Y.; Yamashita, R.; Mizukawa, K.; Saha, M.; Kwan, C.; Moore, C.; Gray, H.; Laursen, D.; Zettler, E.; Farrington, J.; Reddy, C.; Peacock, E.; Ward, M. Organic micro-pollutants in marine plastic debris from the open ocean and remote and urban beaches. *Mar. Pollut. Bull.* **2011**, *62*, 1683–1692.
- (5) Rochman, C. M.; Browne, M. A.; Halpern, B. S.; Hentschel, B. T.; Hoh, E.; Karapanagioti, H. K.; Rios-Mendoza, L. M.; Takada, H.; Teh, S.; Thompson, R. C. Classify plastic waste as hazardous. *Nature* **2013**, *494*, 169–171.
- (6) Rochman, C. M.; Hoh, E.; Hentschel, B. T.; Kaye, S. Long-term field measurement of sorption of organic contaminants to five types of plastic pellets: Implications for plastic marine debris. *Environ. Sci. Technol.* **2013**, *47*, 1646–1654.
- (7) Rochman, C. M. Plastics and priority pollutants: A multiple stressor in aquatic habitats. *Environ. Sci. Technol.* **2013**, *47*, 2439–2440.
- (8) Van, A.; Rochman, C. M.; Flores, E. M.; Hill, K. L.; Vargas, E.; Vargas, S. A.; Hoh, E. Persistent organic pollutants in plastic marine debris found on beaches in San Diego, California. *Chemosphere* **2012**, *86* (3), 258–263.
- (9) Lima, A. L. C.; Farrington, J. W.; Reddy, C. M. Combustion-derived polycyclic aromatic hydrocarbons in the environment—A review. *Environ. Forensics* **2005**, *6* (2), 109–131.
- (10) Harvey, R. G. Environmental chemistry of PAHs. In *PAHs and Related Compounds—Chemistry*; Nielson, A. H., Ed.; Springer: New York, 1998; Vol. 3.1.

- (11) Horii, Y.; Ok, G.; Ohura, T.; Kannan, K. Occurrence and profiles of chlorinated and brominated polycyclic aromatic hydrocarbons in waste incinerators. *Environ. Sci. Technol.* **2008**, *42*, 1904–1909.
- (12) Ma, J.; Horii, Y.; Cheng, J.; Wang, W.; Wu, Q.; Ohura, T.; Kannan, K. Chlorinated and parent polycyclic aromatic hydrocarbons in environmental samples from an electronic waste recycling facility and a chemical industrial complex in China. *Environ. Sci. Technol.* **2009**, *43*, 643–649.
- (13) Lima, A. L. C.; Farrington, J. W.; Reddy, C. M. Combustion-derived polycyclic aromatic hydrocarbons in the environment—A review. *Environ. Forensics* **2005**, *6* (2), 109–131.
- (14) Lohmann, R. Critical review of low-density polyethylene's partitioning and diffusion coefficients for trace organic contaminants and implications for its use as a passive sampler. *Environ. Sci. Technol.* **2012**, *46*, 606–618.
- (15) Dmitrienko, S. G.; Gurariy, E. Y.; Nosov, R. E.; Zolotoz, Y. A. Solid-phase extraction of polycyclic aromatic hydrocarbons from aqueous samples using polyurethane foams in connection with solid-matrix spectrofluorimetry. *Anal. Lett.* **2001**, *34*, 425–438.
- (16) PlasticsEurope. *Plastics—The Facts 2012: An Analysis of European Plastics Production, Demand and Waste Data for 2011*; PlasticsEurope: Brussels, Belgium, 2012; <http://www.plasticseurope.org/Document/plastics-the-facts-2012.aspx?FolID=2>.
- (17) Manzano, C.; Hoh, E.; Simonich, S. L. M. Improved separation of complex polycyclic aromatic hydrocarbon mixtures using novel column combinations in GC × GC/ToF-MS. *Environ. Sci. Technol.* **2012**, *46* (14), 7677–7684.
- (18) Pruter, A. T. Sources, quantities and distribution of persistent plastics in the marine environment. *Mar. Pollut. Bull.* **1987**, *18*, 305–310.
- (19) Carpenter, E.; Anderson, S.; Harvey, G.; Miklas, H.; Peck, B. Polystyrene spherules in coastal waters. *Science* **1972**, *178*, 749–750.
- (20) Lithner, D.; Larsson, A.; Dave, G. Environmental and health hazard ranking and assessment of plastic polymers based on chemical composition. *Sci. Total Environ.* **2011**, *409*, 3309–3324.
- (21) Kitazawa, A.; Amagai, T.; Ohura, T. Temporal trends and relationships of particulate chlorinated polycyclic aromatic hydrocarbons and their parent compounds in urban air. *Environ. Sci. Technol.* **2006**, *40*, 4592–4598.
- (22) Ohura, T.; Kitazawa, A.; Amagai, T.; Makino, M. Occurrence, profiles and photochemical stabilities of chlorinated polycyclic aromatic hydrocarbons associated with particulates in urban air. *Environ. Sci. Technol.* **2005**, *39*, 85–91.
- (23) Wang, W.; Jariyasopit, N.; Schrlau, J.; Jia, Y.; Tao, S.; Yu, T.-W.; Dashwood, R. H.; Zhang, W.; Wang, X.; Simonich, S. L. M. Concentration and photochemistry of PAHs, NPAHs, and OPAHs and toxicity of PM<sub>2.5</sub> during the Beijing Olympic Games. *Environ. Sci. Technol.* **2011**, *45* (16), 6887–6895.
- (24) Manzano, C.; Hoh, E.; Simonich, S. L. M. Quantification of complex polycyclic aromatic hydrocarbon mixtures in standard reference materials using comprehensive two-dimensional gas chromatography with time-of-flight mass spectrometry. *J. Chromatogr., A* **2013**, *1307*, 172–179.
- (25) Allan, I. J.; Booi, K.; Paschke, A.; Vrana, B.; Mills, G. A.; Greenwood, R. Field performance of seven passive sampling devices for monitoring hydrophobic substances. *Environ. Sci. Technol.* **2009**, *43*, 5383–5390.
- (26) Schrap, S. M.; Sleijpen, G. L. G.; Seinen, W.; Opperhuizen, A. Sorption kinetics of chlorinated hydrophobic organic chemicals, Part II. *Environ. Sci. Pollut. Res.* **1994**, *1* (2), 81–92.
- (27) Ravindra, K.; Sokhi, R.; Van Grieken, R. Atmospheric polycyclic aromatic hydrocarbons: Source attribution, emission factors and regulation. *Atmos. Environ.* **2008**, *42* (13), 2895–2921.
- (28) Robinson, A. L.; Donahue, N. M.; Rogge, W. F. Photochemical oxidation and changes in molecular composition of organic aerosol in the regional context. *J. Geophys. Res.* **2006**, *111* (D3), D03302.
- (29) Robinson, A. L.; Subramanian, R.; Donahue, N. M.; Rogge, W. F. Source apportionment of molecular markers and organic aerosol. I. Polycyclic aromatic hydrocarbons and methodology for data visualization. *Environ. Sci. Technol.* **2006**, *40* (24), 7803–7810.
- (30) Rogge, W. F.; Hildemann, L. M.; Mazurek, M. A.; Cass, G. R.; Simoneit, B. R. T. Sources of fine organic aerosol. 2. Noncatalyst and catalyst-equipped automobiles and heavy-duty diesel trucks. *Environ. Sci. Technol.* **1993**, *27* (4), 636–651.
- (31) Guo, H.; Lee, S. C.; Ho, K. F.; Wang, X. M.; Zou, S. C. Particle-associated polycyclic aromatic hydrocarbons in urban air of Hong Kong. *Atmos. Environ.* **2003**, *37* (38), 5307–5317.
- (32) Park, S. S.; Kim, Y. J.; Kang, C. H. Atmospheric polycyclic aromatic hydrocarbons in Seoul, Korea. *Atmos. Environ.* **2002**, *36* (17), 2917–2924.
- (33) Sofowote, U. M.; Allan, L. M.; McCarry, B. E. Evaluation of PAH diagnostic ratios as source apportionment tools for air particulates collected in an urban-industrial environment. *J. Environ. Monit.* **2010**, *12* (2), 417–424.
- (34) Soclo, H. H.; Garrigues, P. H.; Ewald, M. Origin of polycyclic aromatic hydrocarbons (PAHs) in coastal marine sediments: case studies in Cotonou (Benin) and Aquitaine (France) areas. *Mar. Pollut. Bull.* **2000**, *40* (5), 387–396.
- (35) Dickhut, R. M.; Canuel, E. A.; Gustafson, K. E.; Liu, K.; Arzayus, K. M.; Walker, S. E.; Edgecombe, G.; Gaylor, M. O.; MacDonald, E. H. Automotive sources of carcinogenic polycyclic aromatic hydrocarbons associated with particulate matter in the Chesapeake Bay region. *Environ. Sci. Technol.* **2000**, *34*, 4635–4640.
- (36) Sienra, M. Oxygenated polycyclic aromatic hydrocarbons in urban air particulate matter. *Atmos. Environ.* **2006**, *40* (13), 2374–2384.
- (37) Hughes, W. B.; Holba, A. G.; Dzou, L. I. The ratios of dibenzothiophene to phenanthrene and pristane to phytane as indicators of depositional environment and lithology of petroleum source rocks. *Geochim. Cosmochim. Acta* **1995**, *59* (17), 3581–3598.
- (38) Durlak, S. K.; Biswas, P.; Shi, J.; Bernhard, M. J. Characterization of polycyclic aromatic hydrocarbon particulate and gaseous emissions from polystyrene combustion. *Environ. Sci. Technol.* **1998**, *32* (15), 2301–2307.
- (39) Zabanitout, A.; Kassidi, E. Life cycle assessment applied to egg packaging made from polystyrene and recycled paper. *J. Cleaner Prod.* **2003**, *11* (5), 549–559.
- (40) Kwon, E.; Castaldi, M. J. Investigation of mechanisms of polycyclic aromatic hydrocarbons (PAHs) initiated from the thermal degradation of styrene butadiene rubber (SBR) in N<sub>2</sub> atmosphere. *Environ. Sci. Technol.* **2008**, *42*, 2175–2180.
- (41) Wheatley, L.; Levendis, Y. A.; Vouros, P. Exploratory study on the combustion and PAH emissions of selected municipal waste plastics. *Environ. Sci. Technol.* **1993**, *27*, 2885–2895.
- (42) Muller, J. F.; Manomanii, K.; Mortimer, M. R.; McLachlan, M. S. Partitioning of polycyclic aromatic hydrocarbons in the polyethylene/water system. *Fresenius' J. Anal. Chem.* **2001**, *371*, 816–822.
- (43) Pascall, M. A.; Zabik, M. E.; Zabik, M. J.; Hernandez, R. J. Uptake of polychlorinated biphenyls (PCBs) from an aqueous medium by polyethylene, polyvinyl chloride, and polystyrene films. *J. Agric. Food Chem.* **2005**, *53*, 164–169.
- (44) Kirk, R. E.; Othmer, D. F.; Mark, H. F. *Encyclopedia of Chemical Technology*; Interscience Publishers: New York, 1965; Vol. 6.
- (45) Lo, M. T.; Sandi, E. Polycyclic aromatic hydrocarbons (polynuclears) in foods. *Residue Rev.* **1978**, *69*, 35–86.
- (46) Huck, C. W.; Bonn, G. K. Recent developments in polymer-based sorbents for solid-phase extraction. *J. Chromatogr., A* **2000**, *885* (1), 51–72.
- (47) Penner, N. A.; Nesterenko, P. N.; Ilyin, M. M.; Tsyurupa, M. P.; Davankov, V. A. Investigation of the properties of hypercrosslinked polystyrene as a stationary phase for high-performance liquid chromatography. *Chromatographia* **1999**, *50* (9–10), 611–620.
- (48) Kartar, S.; Abou-Seedo, F.; Sainsbury, M. Polystyrene spherules in the Severn estuary—A progress report. *Mar. Pollut. Bull.* **1976**, *7*, 52.